Thin Solid Films 543 (2013) 7–10

Contents lists available at ScienceDirect

Thin Solid Films

journal homepage: www.elsevier.com/locate/tsf

Quantum dot growth on a stripe-pattern

X. Xu, J.-N. Aqua *

Institut des Nanosciences de Paris, Université Pierre et Marie Curie, Paris 6, CNRS UMR 7588, 4 place Jussieu, 75252 Paris, France

ARTICLE INFO

Available online 1 May 2013

Keywords:
Nanostructures
Pattern
Island growth
Epitaxy
Elasticity

ABSTRACT

We study the development of the Asaro-Tiller-Grinfel'd instability on a thin strained film on top of a stripe-patterned substrate and the subsequent growth of self-organized quantum dots. We use a continuum model describing the evolution equation enforced by surface diffusion. We compute the elastic energy up to the first non-linear order and investigate the long time dynamics which describes the dot growth. We find different island locations depending on the substrate wavelength and thickness. As found in experiments, the instability long-time dynamics leads to islands located either on top or in the bottom of the pattern.

1. Introduction

The growth of self-organized islands on a patterned substrate was subject to intense experimental and theoretical works due to their link with application and the fundamental issues concerning growth mechanisms that they address [1–3]. The underlying goal is to achieve a given spatial order and a narrow size distribution which are both limited on a flat substrate, see e.g. [4]. This control is clearly important if one wants to achieve good electrical and optical properties of dots for their potential use in devices.

Of particular interest is the growth of islands on a stripe-patterned substrate. This geometry which is the simplest one may think of, allows to check the control and understanding of island growth on a pattern. However, on the experimental front, no clear scenario emerges as regards to the preferential location of the dots, even in the paradigmatic SiGe systems. Perfectly aligned and regularly spaced one dimensional (1D) arrays of Ge islands appeared on the stripe mesas in [5]. In this work, the pattern was obtained by photolithography and the separation between stripes was 100 nm, similar to the pattern height. This location was also obtained in [6] on larger and sparser stripes. In a slightly different but similar geometry, islands were also found to decorate the top of the undulation resulting from the deposition of a $Si_{1-x}Ge_x$ template layer on a 10° off Si(001) substrate [2]. On the other hand, islands were shown to nucleate in [7] rather on the side of a pattern resulting from holographic lithography and reactive-ion etching, with a period of 500 nm and a height of 100 nm. Finally, in a different but comparable geometry, islands were conversely found in [8] in the bottom of a pit-patterned substrate.

In order to shed some light on the basic mechanisms at work in these systems, we study the evolution of the Asaro-Tiller-Grinfel'd (ATG) instability [9,10] on a pattern. This instability is known to be at work in low-strained SiGe films on Si and corresponds to a nucleationless evolution [11] which finally leads to islands. It must be distinguished with the nucleation of dots in the 2D–3D transition observed in higher strained $Si_{1-x}Ge_x$ films with a higher Ge content, see e.g. [12]. In order to study the instability, we use a basic continuum model which accounts for elasticity, wetting interactions and surface energy. It describes the evolution of the surface morphology as dictated by mass conservation associated with surface diffusion during annealing. We investigate the formation of islands by looking at the long-time evolution of the instability thanks to its non-linear analysis. We find different locations of the dots depending on the pattern wavelength and mean film height. Both parameters rule the external force resulting from the patterned film/substrate interface, especially its amplitude and frequency with respect to the instability characteristic wavelength.

2. Continuum model and non-linear analysis

We use a continuum description relevant to describe the instability dynamics on large scales. We first consider the diffusion equation during annealing

$$\partial h/\partial t = D\Delta_s \mu, \tag{1}$$

where $z = h(r,t)$ is the surface height at time t of the $r = (x,y)$ column, while D is an effective surface diffusion coefficient, Δ_s, the surface Laplacian, and μ, the chemical potential on the surface [13]. Different effects may be accounted for by adding extra terms to the basic chemical potential $\mu = \gamma\kappa + \mathcal{E}^{el}$, where $\mathcal{E}^{el}$ is the elastic energy

* Corresponding author.
E-mail address: aqua@insp.jussieu.fr (J.-N. Aqua).

0040-6090/$ – see front matter
http://dx.doi.org/10.1016/j.tsf.2013.04.089

density on the surface, γ, the surface energy, and κ, the curvature $\kappa = -(h_{xx} + h_{yy}) + \ldots$ at first order in the surface slope. Wetting interactions between the film and the substrate may be accounted for by an explicit dependence of the surface energy on the film thickness [14,15]. The film/substrate interface is patterned and is defined by $z = h_-(r)$, so that we write this dependence as

$$\gamma = \gamma[h(r) - h_-(r)], \tag{2}$$

where we use an exponentially decaying decrease in $\gamma(h)$ [16]. This dependence enforces an additional wetting potential in the chemical potential which merely reads $\Omega\frac{d\gamma}{dh}$, , where Ω is the atomic volume.

In addition to the wetting interactions, the patterned interface also generates buried elastic dipoles which create an elastic field throughout the system. It may be computed by solving the mechanical equilibrium Navier-Cauchy equations $\partial_i\sigma_{ij} = 0$ in the film and in the substrate. An elastic stress is generated by the coherence of their interface and the lattice misfit between them, $m = 1 - a_f/a_s$,, with the film and substrate lattice parameters α_f and α_s. For simplicity, we consider identical elastic properties for the film and substrate. The continuity of forces and displacements at the interface allows us to compute explicitly the solution in the small slope approximation where $|\nabla h_-|$ is supposed to be small. Finally, the film surface is also supposed to be free of stress, which also allows us to compute the full solution for the displacements in the second small slope approximation where $|\nabla h|$ is small. With this solution in hand, one can compute the elastic energy density on the surface $\mathcal{E}^{el} = \mathcal{E}_0 + \mathcal{E}_1 + \mathcal{E}_2 + \ldots$ up to the first non-linear order. At zeroth order in the film and interface slopes, it corresponds to the flat film elastic energy density $\mathcal{E}_0 = Ym^2/(1-\nu)$,, where Y is the film Young modulus and ν, its Poisson ratio. At first order, it is given by [13]

$$\frac{\mathcal{E}_1}{2(1+\nu)\mathcal{E}_0} = -\mathcal{H}_{ii}[h] + \mathcal{B}\{H_{ii}[h_-]\}, \tag{3}$$

with summation over repeated indices and with the generalized Hilbert transforms defined in Fourier space [17]

$$\mathcal{H}_{ij}[h](k) = \frac{k_i k_j}{|k|}\mathcal{F}[h](k), \tag{4}$$

where i, j are either x or y. Moreover, the elastic field created by the buried elastic dipoles at the film/substrate interface is exponentially damped in the growth direction, which is described by the operator

$$\mathcal{B}[h](k) = e^{-|-k|\overline{h}}\mathcal{F}[h](k), \tag{5}$$

with the mean film height $\overline{h} = \langle h\rangle - \langle h_-\rangle$. Finally, considering a 1D pattern parallel to the y-direction $z = h_-(x)$, see Fig. 1, we also computed the elastic energy up to the second order, which can be decomposed in three parts $\mathcal{E}_2 = \mathcal{E}_2^{++} + \mathcal{E}_2^{+-} + \mathcal{E}_2^{--}$, where the first contribution depends only on the upper surface height h contrary to the last one which depends only on the interface h_-, while the second one is an interference term depending on both heights. The first contribution which involves only the film height naturally coincides with the second order computed for a flat film/substrate interface [18]

$$\frac{\mathcal{E}_2^{++}}{2\mathcal{E}_0(1+\nu)} = 2h\Delta h + \left|\nabla h\right|^2 + \mathcal{H}_{ij}[h]\theta_{ijkl}\mathcal{H}_{kl}[h] + 2\mathcal{H}_{ij}\left[h\theta_{ijkl}\mathcal{H}_{kl}[h]\right], \tag{6}$$

where $\theta_{ijij} = 1$ for $i, j = x, y$, $\theta_{iijj} = -\theta_{ijji} = \nu$ for $i \neq j$ while it vanishes otherwise. The new contributions correspond first to the external field associated with the buried dipoles of the film/substrate interface, which merely reads

$$\frac{\mathcal{E}_2^{--}}{2\mathcal{E}_0(1+\nu)} = -\mathcal{B}\left\{\left|\frac{\partial h_-}{\partial x}\right|^2 + h_-\frac{\partial^2 h_-}{\partial x^2}\right\} + \mathcal{B}[\mathcal{H}_{xx}[h_-]]^2, \tag{7}$$

while the cross term which describes the interference between the dipoles of the film surface and the dipoles of the interface is

$$\frac{\mathcal{E}_2^{+-}}{2\mathcal{E}_0(1+\nu)} = -h\mathcal{B}\left[\frac{\partial^2 h_-}{\partial x^2}\right] - 2\mathcal{H}_{xx}[h]\mathcal{B}\mathcal{H}_{xx}[h_-] - 2\nu\mathcal{H}_{yy}[h]\mathcal{B}\mathcal{H}_{xx}[h_-] - 2\mathcal{H}_{xx}\{h\mathcal{B}\mathcal{H}_{xx}[h_-]\} - 2\nu\mathcal{H}_{yy}\{h\mathcal{B}\mathcal{H}_{xx}[h_-]\}. \tag{8}$$

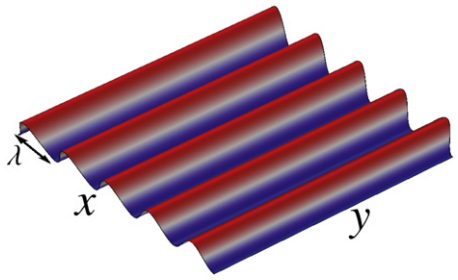

Fig. 1. 1D pattern on which the Asaro-Tiller-Grinfel'd instability develops.

3. Evolution

The characteristic length and time scales are set by the instability driving forces and are given by $l_0 = \gamma_f/2(1+\nu)\mathcal{E}_0$ and $t_0 = l_0^4/D\gamma_f$, where γ_f is the film characteristic surface energy. For a typical $Si_{0.75}Ge_{0.25}$ film on a Si substrate, where the misfit strain is 1%, these are of the order of 27 nm and 25 s [18]. As regards the wetting effect, we consider a smooth exponentially decaying surface energy $\gamma(h) = \gamma_f[1 + c_w exp(-h/\delta_w)]$, where c_w is extrapolated to 0.1, while δ_w is taken as one lattice parameter [18].

The dynamics associated with the evolution Eq. (1) at *linear* order corresponds to the early time dynamics of the instability. In the case of a flat substrate and without wetting interactions, a perturbation with a wave-vector vk grows exponentially with time with the ATG growth rate $\sigma = |k|^3 - k^4$ in dimensionless units defined with l_0 and t_0 [9,10]. This growth rate displays a maximum for a given $|k|$, which allows to define the instability characteristic length scale λ_{ATG}. When wetting interactions are acting, an extra $-k^2e^{-h/\delta_w}$ term is present and enforces a negative σ for $h < h_c$, below which a thin film remains stable and does not develop the morphological instability. The evolution at linear order with the initial condition (9) and the pattern influence (Eq. (3)) was analyzed in Ref. [13] for a similar but slightly different 2D egg-carton shape. Kinetic phase diagrams were exhibited, which describe the surface geometry as a function of the pattern wavelength λ, the film thickness $\overline{h}$ and the duration t of the evolution. Three main configurations were found. In the first two, the film displays mainly the pattern shape but is either in-phase (the maxima of the film lie on top of the maxima of the substrate) or out-of-phase (the film and substrate maxima and minima lie on top of each other). A continuous transition from the initial in-phase to the energy-minimizing out-of-phase configurations was evidenced, which occurs by the vanishing of the film roughness in order to allow the phase shift even for a positive growth rate [13]. The last film geometry which may be found in the linear analysis, is associated with the 'classic' ATG instability shape, well-defined in Fourier space by a ring of maxima which correspond to the wavevectors which maximize the linear growth rate. In this last case, the influence of the pattern may be quantified in Fourier space, but is hardly visible in real space.

To go beyond the initial linear evolution, we numerically solve the non-linear evolution Eq. (1) using a pseudo-spectral method devised to stiff non-linear partial differential equations [19]. We consider an